JOC*Article*

A Quenched Molecular Dynamics−Rotating Frame Overhauser Spectroscopy Study of a Series of Semibiosynthetically Monoacylated Anthocyanins†

Neil A. Whittemore,‡,§ Karen T. Welch,‡,§ James R. Cox,‡,∥ Donald K. Dougall,⊥ and David C. Baker*,‡

Departments of Chemistry and Botany, The University of Tennessee, Knoxville, Tennessee 37996

dcbaker@utk.edu

Received September 20, 2003

Quenched molecular dynamics (QMD), in conjunction with NMR (ROESY) studies, was used to investigate the conformational behavior of some semibiosynthetic anthocyanins of the type 6-*O*-acyl-*β*-D-Glc*p*-(166)-*β*-D-Gal*p*-(1→O^3)-cyanidin, with and without a *β*-D-Xyl*p* branch at the 2-*O*-Gal position. These compounds, which are produced by the addition of selected carboxylic acids to growing tissue cultures of *Daucus carota* (wild carrot), are of interest as color-stabilized anthocyanins, some of which have potential as useful colorants in the nutraceutical and pharmaceutical industries. The QMD−ROESY studies, performed for the first time on anthocyanins, have led to the identification of families of conformers of these flexible molecules that are of interest in work toward determining the mechanism for stabilization of color among these compounds in solution.

Introduction

Since the pioneering work of Richard Willstäter in the early 20th century on the chemistry of anthocyanins,[1] these compounds have been recognized as important colorants in nature. Currently, the colorants used in the food, pharmaceutical, and nutraceutical industries are, for the most part, synthetic compounds and have come under increasing scrutiny in recent years for their safety. Among the possible replacements for these synthetic colorants are the anthocyanins, which are the compounds responsible for most of the nongreen coloration in plants. These compounds are responsible for the coloring of apples, strawberries, grapes, red cabbage, as well as for the reds, blues, and purples of flowers. Structurally, anthocyanins have both aglycon (flavylium) and glycon domains (refer to Figure 1). It is the flavylium chromophore that is responsible for the intense color observed when these compounds are dissolved in an aqueous medium. However, loss of their vivid color in solution is the result of the attack of water at the C-2 flavylium position at near-neutral pH.[2,3] While reviews in the field indicate that industrial interest for anthocyanins is high,[3,4] there is only limited use of these compounds at the present time, mainly due to the fact that these compounds (a) are of limited availability and (b) many lose their color at or near neutral pH, precluding their use in most foodstuffs.

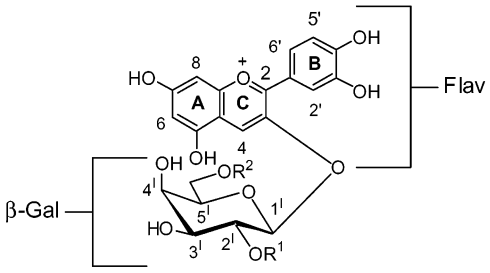

1	R^1 = β-Xyl	R^2 = β-Glc	R^3 = 3,4,5-(OMe)$_3$-Cin
2	R^1 = H	R^2 = β-Glc	R^3 = 3,4,5-(OMe)$_3$-Cin
3	R^1 = β-Xyl	R^2 = β-Glc	R^3 = 4-F-Cin
4	R^1 = β-Xyl	R^2 = β-Glc	R^3 = 3,4,5-(OMe)$_3$-Bz
5	R^1 = β-Xyl	R^2 = β-Glc	R^3 = H

FIGURE 1. Structures of the anthocyanins under study.

* To whom correspondence should be addressed. Phone: (865) 974-1066. Fax: (865) 974-1536.

† Studies on the Stability and Conformation of Monoacylated Anthocyanins. 4. Part 3: see ref 20.

‡ Department of Chemistry.

§ Current address: Department of Biochemistry and Cellular and Molecular Biology, The University of Tennessee, Knoxville, TN 37996.

∥ Current address: Department of Chemistry, Murray State University, Murray, KY 40271.

⊥ Department of Botany.

(1) Willstätter, R.; Everest, A. E. *Justus Liebigs Ann. Chem.* **1913**, *401*, 189−232.

(2) Brouillard, R. In *Anthocyanins as Food Colors*; Markakis, P., Ed.; Academic Press: New York, 1982; pp 1−40.

(3) Mazza, G.; Miniati, E. *Anthocyanins in Fruits, Vegetables, and Grains*; CRC Press: Boca Raton, FL, 1993.

(4) Francis, F. J. *CRC Crit. Rev. Food Sci. Nutr.* **1989**, *28*, 273−314.

10.1021/jo035380w CCC: $27.50
Published on Web 02/05/2004

A new class of semibiosynthetic monoacylated anthocyanins produced by tissue cultures of the wild carrot, *Daucus carota*, were prepared[5] to specifically examine the nature of the intramolecular interactions between the acyl moiety—cinnamoyl or benzoyl—and the glycon subunits, which play a role in the mechanisms involved in the observed color loss. The biosynthetic process is carried out by adding cinnamic or benzoic acids to the tissue cultures and harvesting the products that are acylated at the O-6 Glc terminus. This produces compounds that are of the structure 6-*O*-acyl-*β*-D-Glc*p*-(1→6)-*β*-D-Gal*p*-(1→O[3])-cyanidin, with and without a *β*-D-Xyl*p* branch at the 2-*O*-Gal position, with a range of color stabilities. To investigate the mechanism for color stabilization, five compounds, four with the 2-*O*-*β*-D-Xyl branch, including nonacylated compound **5**, and three compounds where acyl = 3,4,5-trimethoxycinnamoyl (**1**), 4-fluorocinnamoyl (**3**), and 3,4,5-trimethoxybenzoyl (**4**), plus compound **2**, which is **1** that lacks the 2-*O*-*β*-D-Xyl (see Figure 1), were selected for study. The advantage of studying these anthocyanins over studying naturally occurring monoacylated anthocyanins is that diverse acyl moieties (supplied as substituted or unsubstituted cinnamic or benzoic acids)[5] could be programmed into the synthetic sequence, which would allow details of the mechanisms for color loss to be thoroughly dissected by molecular modeling and by analysis of stereoelectronic effects. To achieve these goals, a general molecular modeling protocol is required that would permit the construction of reasonable models of these five, highly flexible, monoacylated anthocyanins in methanol.

We now report our findings that a quenched molecular dynamics (QMD)[6−16] protocol can be used to achieve this requirement for a series of five semibiosynthetically prepared anthocyanins. We show that the QMD protocol, in concert with data acquired in 2D NMR studies, yields families of structures rather than a single structure (which has been the norm for modeling anthocyanins) for each anthocyanin studied.[17−19] Details of the QMD studies, which are the first reported for anthocyanins, are provided herein. Eventually these investigations are anticipated to lead to the rational design of a monoacylated anthocyanin that is color stable and could be commercially produced by our semibiosynthetic process.[5]

Results and Discussion

Isolation, Purification, and Characterization. (a) General Procedures. The semibiosynthetic anthocyanins used in this study were isolated, purified, and characterized according to the procedures described in the paper by Dougall et al.[5] For this method-development study it was of paramount importance to select five anthocyanins of a range of color stabilities that would permit the thorough examination of the mechanisms that cause color loss from hydration at C-2. Thus, the equilibrium constants for the hydration reaction (K_h) were determined by the methods that were detailed in the work by Redus et al.[20] The five compounds **1**−**5** were judiciously selected for use in the QMD study; anthocyanins **1** and **2** were the most color stable, progressing through to anthocyanin **5**, which was the least color stable of the semibiosynthetic anthocyanins currently tested.

(b) 1D and 2D ^{1}H NMR Studies. 1D ^{1}H NMR spectra were obtained on compounds **1**−**5** in methanol-d_4 as described in the work by Dougall et al.[5] Methanol was selected for its demonstrated good NMR spectral dispersion and its high polarity (close to that of water), as well as for the fact that methanol had been the solvent of choice in earlier studies.[21−23] Concentrations of the studied compounds were such that in 1D ^{1}H NMR studies no aggregation was observed.[24] To obtain NMR-derived restraints to validate structures produced from the QMD protocol, data derived from rotating frame Overhauser spectroscopy (ROESY)[25] were needed. To establish the optimal mixing time, several ROESY spectra were obtained for compound **3** with mixing times between 50 and 750 ms. It was determined that the optimal mixing time was found to be 500 ms, and this was applied to compounds **1**−**5**. With all of the ^{1}H assignments for these compounds complete,[5] the cross-peaks were easily correlated to specific proton−proton distances. Examples of these NMR-derived restraints for **1** are shown in Figure 2. The interactions represented by a, b, and c in Figure 2 are between H-7^D and H-1^I, H-4 and H-1^I, and H-7^D and H-2^I, respectively. The total number of rotating frame Overhauser effects (ROEs) for the five compounds under investigation were 18, 10, 22, 20, and 15 for compounds

(5) Dougall, D. K.; Baker, D. C.; Gakh, E. G.; Redus, M. A.; Whittemore, N. A. *Carbohydr. Res.* **1998**, *310*, 177−189.
(6) Pettitt, B. M.; Matsunaga, T.; al-Obeidi, F.; Gehrig, C.; Hruby, V. J.; Karplus, M. *Biophys. J.* **1991**, *60* , 1540−1544.
(7) O'Connor, S. D.; Smith, P. E.; al-Obeidi, F.; Pettitt, B. M. *J. Med. Chem.* **1992**, *35*, 2870−2881.
(8) Altomare, C.; Cellamare, S.; Carotti, A.; Casini, G.; Ferappi, M.; Gavuzzo, E.; Mazza, F.; Carrupt, P. A.; Gaillard, P.; Testa, B. *J. Med. Chem.* **1995**, *38*, 170−179.
(9) Burgess, K.; Ho, K.-K.; Pettitt, B. M. *J. Am. Chem. Soc.* **1995**, *117*, 54−65.
(10) Burgess, K.; Ho, K.-K.; Pal, B. *J. Am. Chem. Soc.* **1995**, *117*, 3808−3819.
(11) Burgess, K.; Ke, C.-Y. *J. Pept. Res.* **1997**, *49*, 201−209.
(12) Cutts, R. J.; Howlin, B. J.; Mulholland, F.; Webb, G. A. *J. Agric. Food Chem.* **1996**, *44*, 1409−1415.
(13) Burgess, K.; Lim, D.; Mousa, S. A. *J. Med. Chem.* **1996**, *39*, 4520−4526.
(14) Lim, D.; Burgess, K. *J. Am. Chem. Soc.* **1997**, *119*, 9632−9640.
(15) Al-Obeidi, F.; O'Connor, S. D.; Job, C.; Hruby, V. J.; Pettitt, B. M. *J. Pept. Res.* **1998**, *51*, 420−431.
(16) Ashish, K. R. *Bioorg. Med. Chem.* **2002**, *10*, 4083−4090.
(17) Whittemore, N. A. I. Conformational Studies of Monoacylated Anthocyanins: Factors That Affect Their Color Stability. II. Design and Synthesis of Electroactive Oligodeoxynucleotides. Probes for Nucleic Acid Hybridization. Ph.D. Dissertation, University of Tennessee—Knoxville, Knoxville, TN, 1999.
(18) Welch, K. T.; Whittemore, N. A.; Baker, D. C.; Dougall, D. K. Conformational Studies of Monoacylated Anthocyanins: Factors That Affect Their Color Stability. *Abstracts of Papers*, 219th National Meeting of the American Chemical Society, San Francisco, CA, March 26−30, 2000; American Chemical Society: Washington, DC, 2000; CARB-066.
(19) Welch, K. T. Conformational Studies of Carbohydrates and Carbohydrate-containing molecules. Ph.D. Dissertation, University of Tennessee—Knoxville, Knoxville, TN, 2002.
(20) Redus, M.; Baker, D. C.; Dougall, D. K. *J. Agric. Food Chem.* **1999**, *47*, 3449−3454.
(21) Goto, T.; Kondo, T. *Angew. Chem., Int. Ed. Engl.* **1991**, *30*, 17−33, and references therein.
(22) Nerdal, W.; Anderson, Ø. M. *Phytochem. Anal.* **1991**, *2*, 263−270.
(23) Nerdal, W.; Anderson, Ø. M. *Phytochem. Anal.* **1992**, *3*, 182−189.
(24) Gakh, E. G.; Dougall, D. K.; Baker, D. C. *Phytochem. Anal.* **1998**, *9*, 28−34.
(25) Hwang, T.-L.; Shaka, A. J. *J. Am. Chem. Soc.* **1992**, *114*, 3157−3159.

TABLE 1. NMR-Derived Restraints of Anthocyanin 1 in Methanol-d_4

proton−proton pair	vol measured ($\times 10^6$)	strength of interaction[a]	proton−proton pair	vol measured ($\times 10^6$)	strength of interaction[a]
H-8^{D}−H-2^{D}	3.8	S	H-7^{D}−H-2^{I}	0.61	W
H-8^{D}−H-6^{D}	3.8	S	H-4−H-2^{I}	0.48	W
H-6^{IIIA}−H-6^{IIIB}	3.2	S	H-1^{I}−H-4^{I}	0.27	W
H-7^{D}−H-2^{D}	2.6	M	H-1^{I}−H-5^{I}	0.034	W
H-7^{D}−H-6^{D}	2.6	M	H-4^{I}−H-3^{I}	*b*	W
H-4^{I}−H-5^{I}	1.01	W	H-4−H-3^{I}	*b*	W
H-4^{I}−H-2^{I}	0.91	W	H-7^{D}−H-3^{I}	*b*	W
H-7^{D}−H-1^{I}	0.8	W	H-7^{D}−H-8^{D}	*b*	W
H-4−H-1^{I}	0.78	W	H-4^{II}−H-5^{IIA}	*b*	W

[a] Strong interaction (S) = 1.7−2.5 Å; medium interaction (M) = 1.7−3.2 Å; weak interaction (W) = 1.7−5 Å. [b] An ROE was confirmed by visual inspection of the spectrum, but its volume could not be measured accurately due to either t_1 noise or overlap of signals. All these are assigned as weak interactions.

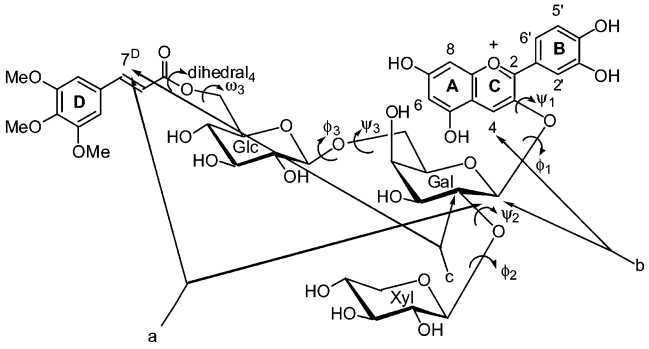

FIGURE 2. Dihedral angles and long-distance restraints for **1**. The interactions are as follows: a, H-7^{D}−H-1^{I}; b, H-4−H-1^{I}; c, H-7^{D}−H-2^{I}.

1−**5**, respectively. These ROEs were sorted into categories: strong (1.7−2.5 Å), medium (1.7−3.2 Å), and weak (1.7−5.0 Å). These restraints varied from interactions within the subunits of the anthocyanin molecular structure to interactions between remote parts of the molecular structure, H-6^{IIIA}−H-6^{IIIB} and H-4−H-2^{I}, respectively. All the NMR-derived restraints used for **1** are shown in Table 1; all other tables of data and figures showing all the families observed for compounds **2**−**5** are provided in the Supporting Information.

Molecular Modeling Studies. (a) QMD Studies. Over the past few years, QMD has been used to produce reasonable molecular structures of a variety of peptides, such as a cyclic enkephalin analogue,[6] tuftsin and cyclic analogues,[7] the piracetam-type nootropics,[8] small peptides that contain highly constrained amino acids,[9−11] the Delicious Peptide,[12] spirocyclic peptidomimetics,[13,14] linear and cyclic α-melanotropins,[15] and most recently an immunostimulating tetrapeptide, rigin.[16] Simply, the automated QMD protocol used in this study was adopted from the work of Burgess and co-workers[9−11,13] and involves the capture of molecular coordinates throughout a 1 ns trajectory of molecular dynamic simulation. The captured coordinates are then subjected to an exhaustive minimization in a dielectric continuum of methanol to a root-mean-square (RMS) energy derivative of 0.0001 kcal Å^{-1}. Thus, for each compound investigated the QMD protocol produced 1000 structures. For this QMD protocol to succeed, it was imperative that the conformational space be thoroughly explored, which would prevent the entrapment in local energy minima. Figure 3a shows a plot of ϕ_1 vs ψ_1 (for the definition of the dihedral angles, refer to Figure 2) for the 1000 structures following the molecular dynamics simulation of **1**. Figure 3b is essentially the same plot, but one that uses the structures after exhaustive minimization. Similar plots of the other dihedral angles, which are defined in Figure 2, are supplied as Figures S1−S6 in the Supporting Information. It was apparent that the coordinates of compound **1** were randomized in the initial simulation; however, after the resulting structures were minimized, no single conformation was shown to dominate, but discrete conformational families were observed. These structures were screened further by rejecting any structures that were ≥5 kcal Å^{-1} greater than the global minimum energy for the assembly of structures. For a summary of the results, refer to Table 2. To further select the most reasonable structure, the NMR-derived restraints from Table 1 were used.

(b) Structural Families of Semibiosynthetic Monoacylated Anthocyanins. When each assembly of structures for **1**−**5** (651, 368, 535, 257, and 886 structures, respectively) was visually inspected, it was evident that distinct conformational families had been generated by the QMD protocol employed in this study. Conformational families were defined by the orientation of the subunits within each conformer.

For instance, the **F3** family for **1**−**3**, i.e., **1F3**, **2F3**, and **3F3**, is shown in Figure 4. The conformers shown are the representative structures that had the lowest energy and the least number of violations, particularly among long-distance restraints. Each conformer is oriented in the same manner, by sighting down the C-2−C-3 bond in the C ring of the Flav nucleus and placing the Gal residue behind the Flav nucleus. Initially, the families were defined on the basis of how the Flav nucleus is read from left to right. In Figure 5 Flav is read as "B−CA", whereas in some families the nucleus can be read "AC−B" (refer to Figure 6 for examples of these families of **1**). The next aspect of defining these structures that was considered was the alignment of the O-6 position of the β-Gal that is glycosylated with β-Glc. The β-Glc moiety was forced to be positioned to either the left or the right or underneath the Flav residue. Further, conformers were grouped into families on the basis of the location of the cinnamoyl unit (cyan) under the flavylium nucleus (AC moiety, magenta; B ring, yellow). Thus, family **F3** represents structures where the Flav is read as B−CA, the β-Glc moiety is "forced" to the right, and finally the acyl ring is positioned to interact with the AC ring. Despite the fact that these three structures shown in Figure 4 are of three different compounds, clearly the

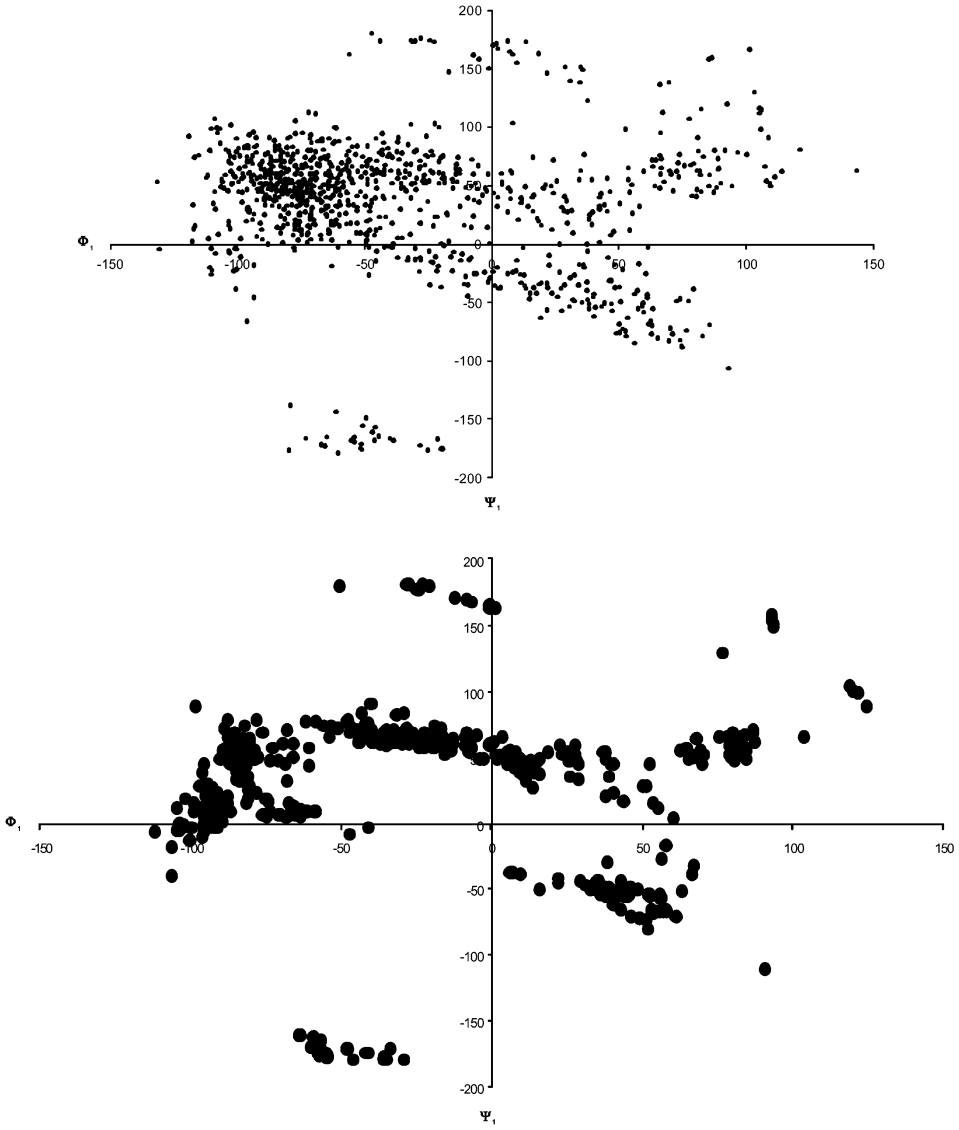

FIGURE 3. (a, top) A plot of ϕ_1 vs ψ_1 of 1000 structures of **1** after 1 ns molecular dynamics at 600 K. (b, bottom) A plot of ϕ_1 vs ψ_1 of 1000 structures of **1** after minimization.

TABLE 2. Summary of Data Obtained from the QMD−ROESY Study of Anthocyanins 1−5 in a Dielectric Continuum of Methanol

compd[a]	no. of families	total energy (kcal Å^{-1})	no. NMR-derived restraints satisfied
1 (651)	11	196.8 ± 1.5	≥12
2 (368)	5	188.1 ± 1.3	≥7
3 (535)	6	174.3 ± 1.3	≥16
4 (257)	8	196.8 ± 1.6	≥17
5 (886)	5	142.3 ± 1.1	≥10

[a] The number in parentheses represents the total number of structures that are within 5 kcal Å^{-1} of the global minimum and satisfy the NMR-derived restraints.

structures shown demonstrate a similar conformation for family **F3**. For each conformer in each family, the dihedral angles ϕ_1, ψ_1, ϕ_2, ψ_2, ϕ_3, and ω_3, which are shown in Figure 2, were determined. Tables 3−7 summarize the results obtained in this initial analysis of compounds **1**−**5**. To highlight the observations for all the anthocyanins in this study, all the conformational families for **1** are shown in Figures 5 and 6. Each family is oriented in the same manner as described earlier. Of particular

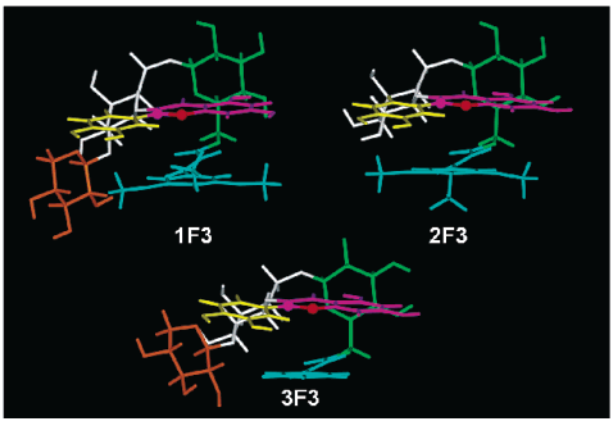

FIGURE 4. Representative structures of the **1F3**, **2F3**, and **3F3** families. In each structure the AC ring is magenta, the B ring is yellow, β-Gal is white, β-Xyl is orange, β-Glc is pale green, and the acyl moiety is cyan.

interest is that, for all the families in Figure 5, the rings that compose the Flav nucleus are read from left to right,

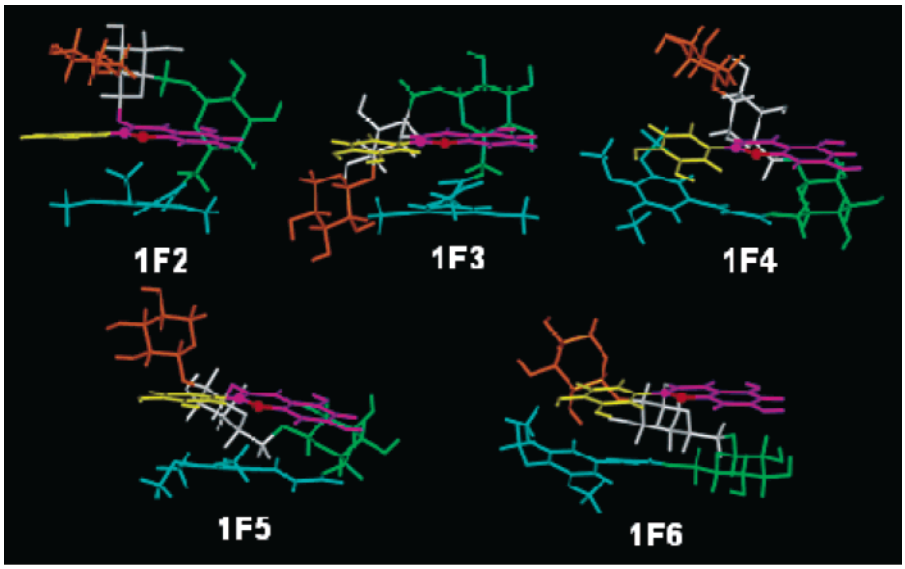

FIGURE 5. Representative structures of the **1F2**, **1F3**, **1F4**, **1F5**, and **1F6** families. In each structure the AC ring is magenta, the B ring is yellow, β-Gal is white, β-Xyl is orange, β-Glc is pale green, and the acyl moiety is cyan.

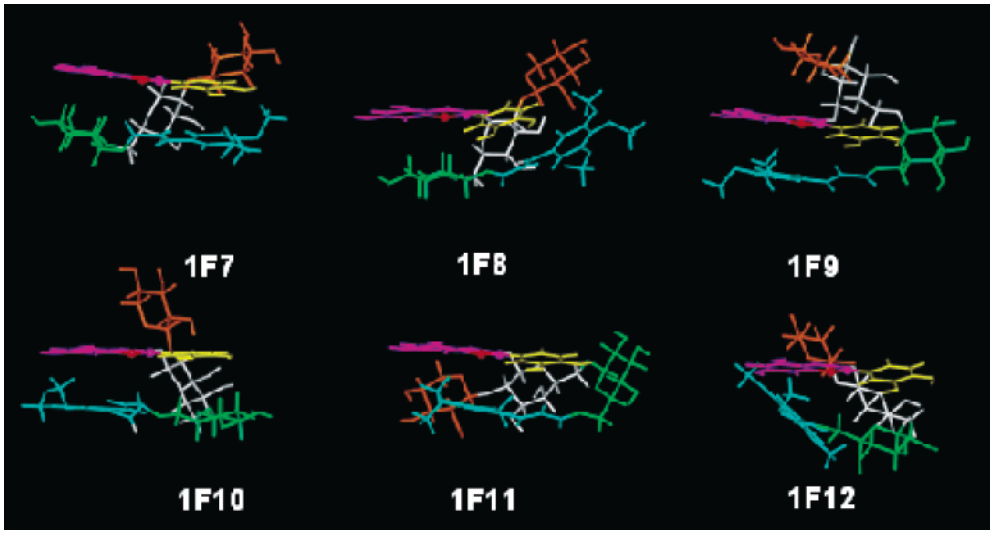

FIGURE 6. Representative structures of the **1F7**, **1F8**, **1F9**, **1F10**, **1F11**, and **1F12** families. In each structure the AC ring is magenta, the B ring is yellow, β-Gal is white, β-Xyl is orange, β-Glc is pale green, and the acyl moiety is cyan.

TABLE 3. Dihedral Angles (deg) of the Families of Anthocyanin 1

conformational family[a]	av energy (kcal Å^{-1})	ϕ_1[b,c]	ψ_1	ϕ_2	ψ_2	ϕ_3	ω_3	no. of restraints met	RMSD
1F2 (9)	198 ± 1	−173 ± 4	−57 ± 2	55 ± 2	28 ± 2	46 ± 2	−56 ± 3	12/16	1.3 ± 0.9
1F3 (6)	198 ± 1	37 ± 4	20 ± 6	49 ± 14	30 ± 4	53 ± 1	−55 ± 2	15/16	0.9 ± 0.1
1F4 (69)	199	178 ± 6	−28 ± 12	60 ± 2	9 ± 7	11 ± 18	52 ± 1	13/16	2.2 ± 0.7
1F5 (59)	198 ± 1	63 ± 1	83 ± 2	39 ± 27	−9 ± 5	47 ± 3	43 ± 11	13/16	1.2 ± 0.8
1F6 (316)	196 ± 1	49 ± 3	76 ± 7	29 ± 23	10 ± 7	27 ± 14	55 ± 2	13/16	1.8 ± 0.7
1F7 (1)	199	72	−37	46	24	60	58	14/16	
1F8 (74)	198 ± 1	67 ± 2	−35 ± 2	21 ± 10	−1 ± 8	81 ± 3	59 ± 5	12/16	1.6 ± 0.8
1F9 (3)	199	−60 ± 10	49 ± 7	64 ± 5	19 ± 6	43 ± 22	19 ± 71	13/16	2.0 ± 0.1
1F10 (59)	198 ± 1	46 ± 10	−84 ± 4	49 ± 39	−17 ± 16	41 ± 6	47 ± 3	12/16	1.3 ± 0.6
1F11 (1)	198	−37	−112	50	30	55	−49	15/16	
1F12 (54)	196 ± 1	6 ± 6	−94 ± 3	35 ± 36	−4 ± 7	16 ± 10	56 ± 3	15/16	2.1 ± 0.7

[a] The number in parentheses is the total number of structures in the individual families. [b] Angle values that have no errors indicated in the table have an error less than ±0.5°. [c] The dihedral angles are defined in Figure 2.

B, C, and A, whereas in Figure 6 the rings are read A, C, and B. Another observation within this group of 11 families was the varied position of the 3,4,5-trimethoxycinnamoyl ring irrespective of the orientation of the Flav nucleus. In families **1F2**, **1F3**, **1F9**, **1F10**, and **1F11**, the acyl unit (cyan) is located directly under the AC rings

TABLE 4. Dihedral Angles (deg) of the Families of Anthocyanin 2

conformational family[a]	av energy (kcal Å^{-1})	ϕ_1[b,c]	ψ_1	ϕ_2	ψ_2	ϕ_3	ω_3	no. of restraints met	RMSD
2F3 (55)	189 ± 1	37 ± 8	11 ± 2	−	−	53 ± 3	−55 ± 3	8/8	1.0 ± 0.6
2F5 (13)	189 ± 1	69 ± 9	86 ± 3	−	−	48 ± 3	45 ± 3	8/8	1.1 ± 0.6
2F6 (76)	189 ± 1	38 ± 4	67 ± 7	−	−	18 ± 14	55 ± 2	8/8	2.2 ± 0.7
2F10 (171)	187 ± 1	52 ± 4	−86 ± 2	−	−	40 ± 2	46 ± 5	7/8	1.8 ± 0.8
2F12 (53)	189 ± 1	−6 ± 12	−96 ± 3	−	−	15 ± 12	53 ± 5	8/8	1.6 ± 0.9

[a] The number in parentheses is the total number of structures in the individual families. [b] Angle values that have no errors indicated in the table have an error less than ±0.5°. [c] The dihedral angles are defined in Figure 2.

TABLE 5. Dihedral Angles (deg) of the Families of Anthocyanin 3

conformational family[a]	av energy (kcal Å^{-1})	ϕ_1[b,c]	ψ_1	ϕ_2	ψ_2	ϕ_3	ω_3	no. of restraints met	RMSD
3F3 (10)	177	40 ± 9	25 ± 20	26 ± 14	32 ± 18	34 ± 21	−10 ± 55	18/20	1.5 ± 0.5
3F4 (1)	177	178	−28	9	60	32	52	16/20	
3F6 (25)	174 ± 1	49 ± 3	78 ± 5	11 ± 9	−18 ± 48	28 ± 13	54 ± 3	18/20	1.1 ± 0.4
3F10 (9)	175 ± 1	52 ± 4	−86 ± 1	−19 ± 17	43 ± 30	41 ± 2	48 ± 2	17/20	0.9 ± 0.3
3F11 (197)	176	−36 ± 7	−113 ± 1	29 ± 1	46 ± 13	51± 14	−38 ± 33	18/20	0.8 ± 0.5
3F12 (293)	174 ± 1	8 ± 6	−93 ± 2	−5 ± 9	24 ± 41	19 ± 11	56 ± 4	19/20	1.3 ± 0.4

[a] The number in parentheses is the total number of structures in the individual families. [b] Angle values that have no errors indicated in the table have an error less than ±0.5°. [c] The dihedral angles are defined in Figure 2.

TABLE 6. Dihedral Angles (deg) for the Families of Anthocyanin 4

conformational family[a]	av energy (kcal Å^{-1})	ϕ_1[b,c]	ψ_1	ϕ_2	ψ_2	ϕ_3	ω_3	no. of restraints met	RMSD
4F1 (23)	198	−20	−106	27	58	49	−24	17/18	0.6 ± 0.1
4F2 (16)	198	−163	−56 ± 2	26 ± 1	61 ± 3	55 ± 5	−47 ± 8	17/18	1.6 ±0.3
4F3 (10)	198	32 ± 1	42	34	55 ± 1	46 ± 1	33 ± 2	18/18	0.6 ± 0.1
4F9 (63)	198	−48 ± 7	33 ± 11	7 ± 7	68	42 ± 7	72 ± 44	17/18	0.8 ± 0.7
4F10 (99)	198	47 ± 18	−79 ± 10	−19 ± 17	40 ± 15	40 ± 2	77 ± 1	18/18	0.9 ± 0.3
4F11 (2)	198	−14	−102	24	53	55	−33	18/18	0.7
4F12 (69)	195 ± 1	−1 ± 8	−96 ± 3	8 ± 14	33 ± 36	23 ± 4	87 ± 3	18/18	1.1 ± 0.3
4F16 (5)	199	35°	37 ± 9	25 ± 31	45 ± 36	49 ± 1	−31 ± 2	17/18	0.8 ± 0.4

[a] The number in parentheses is the total number of structures in the individual families. [b] Angle values that have no errors indicated in the table have an error less than ±0.5°. [c] The dihedral angles are defined in Figure 2.

TABLE 7. Dihedral Angles (deg) for the Families of Anthocyanin 5

conformational family[a]	av energy (kcal Å^{-1})	ϕ_1[b,c]	ψ_1	ϕ_2	ψ_2	ϕ_3	ω_3	no. of restraints met	RMSD
5F8 (198)	143 ± 1	73 ± 3	−65 ± 8	−8 ± 13	51 ± 27	−50 ± 7	−	11/15	1.2 ± 0.6
5F12 (61)	142 ± 1	16 ± 4	−89 ± 1	−7 ± 9	48 ± 42	28 ± 2	−	12/15	0.8 ± 0.3
5F13 (55)	143 ± 1	56 ± 3	−90 ± 1	−18 ± 19	−93 ± 82	52 ± 5	−	10/15	0.9 ± 0.4
5F14 (155)	143 ± 1	67 ± 6	−83 ± 1	−13 ± 17	43 ± 15	45 ± 3	−	10/15	0.8 ± 0.3
5F15 (417)	141 ± 1	60 ± 2	−78 ± 2	−15 ± 19	48 ± 32	40 ± 1	−	10/15	0.9 ± 0.3

[a] The number in parentheses is the total number of structures in the individual families. [b] Angle values that have no errors indicated in the table have an error less than ±0.5°. [c] The dihedral angles are defined in Figure 2.

(magenta), while, in **1F4**, **1F5**, and **1F7**, the cinnamoyl unit (cyan) overlaps the B ring (yellow) of the Flav core. Additionally, there are three families, **1F6, 1F8**, and **1F12**, where the aromatic residue (cyan) is in "no man's land" with no obvious interactions with other subunits of **1**. The final observation was that of the various positions that were adopted by the Xyl subunit (orange) in both families in Figures 5 and 6. Rather than a conformational family for each compound being obtained, several distinct families were produced from the QMD−ROESY study. The variety of conformational families of structures was undoubtedly dictated by the apparent $\pi-\pi$ (cinnamoyl−Flav)[26] and carbohydrate−arene interactions.[27,28]

The conformational families observed for compound **1** (most color stable) and **3** (less color stable; for conformational families, see Figure S8 in the Supporting Information) demonstrate that the fold of each of the conformational families is very similar. This phenomenon is readily observed in the depiction of family **F3** in Figure 4. Thus, the shapes of the molecules cannot be used alone to explain the varied color stabilities observed. If this were the case, all cinnamoylated anthocyanins would have similar color stability properties, which they obviously do not.[20] However, these solution-based models could be used to probe the subtle nature of the intramolecular stereoelectronic factors involved in color stability processes.

The QMD protocol described herein, which for the first time has been applied to anthocyanins, yielded a general molecular modeling protocol for these highly flexible,

(26) Hunter, C. A.; Sanders, J. K. M. *J. Am. Chem. Soc.* **1990**, *112*, 5525−5534.
(27) Choe, B. Y.; Ekborg, G. C.; Rodén, L.; Harvey, S. C.; Krishna, N. R. *J. Am. Chem. Soc.* **1991**, *113*, 3743−3749.
(28) Qasba, P. K. *Carbohydr. Polym.* **2000**, *41*, 293−309.

semibiosynthetic anthocyanins. This methodology, which generates families of conformers as opposed to single structures, will be applied to other novel anthocyanins produced in our laboratory to extend our understanding of the chemistry of these potentially useful colorants. Ultimately our goal is the rational design of highly color stable, semibiosynthetic monoacylated anthocyanins that can be used as colorants in the pharmaceutical and nutraceutical industries.

Experimental Section

General Procedures. Except as described below, all procedures are the same as described by Dougall et al.[5]

Determination of Equilibrium Constants. These were performed as described in the work of Dougall and co-workers.[20]

NMR Studies. The samples were prepared and characterized according to Dougall et al.[5] ROESY experiments on the anthocyanins in methanol-d_4 were performed as follows. A ROESY spectrum[25] was acquired at 400 MHz at 293 K. In the ROESY experiments, a total of 256 FIDs of 2K datapoints were collected with a total of 64 scans per FID with a spectral width of 3205 Hz. The data were zero-filled to 1K points in t_1 and multiplied by the sine^2 window function in both dimensions before Fourier transformation. The choice of a mixing time of 500 ms was used, and the transmitter offset was placed on the H_2O resonance, which was irradiated with a lower power pulse during a relaxation delay of 2 s to suppress the water signal. The offset frequency was optimized for each compound. All processing was performed with FELIX 95 software (Accelrys, San Diego, CA) on a Silicon Graphics Indigo2 workstation. Processing was performed as previously described for the ROESY experiments. The volumes of all the cross-peaks were measured in the Felix 95 NMR processing program. For the structure validation for **1**−**5**, the ROEs were categorized as strong (1.7−2.5 Å), medium (1.7−3.2 Å), and weak (1.7−5.0 Å).

Molecular Modeling Studies. (a) General Procedures. All molecular mechanics and molecular dynamics calculations were accomplished with the CVFF force field[29] interfaced with Insight II/Discover (Accelerys) operating on a Silicon Graphics Indigo^2 workstation. All calculations were carried out in vacuo with a dielectric continuum of 32.6 to mimic methanol. Molecular dynamics calculations were carried out using the Verlet Leapfrog Integrator using a time step of 1 fs and an equilibration time of 0.1 ps. All simulations were done at constant temperature under canonical ensemble (NVT) conditions.

(b) QMD Studies. QMD simulations were carried out using the general protocol of Burgess and co-workers to treat flexible molecules.[13,14] A random structure of each anthocyanin **1**−**5** was subjected to conjugate gradient minimization until the RMS energy derivative was less than 0.0001 kcal Å^{-1}. The structure was then heated from 300 to 600 K over 30 ps by increasing the temperature by 10 K every 1 ps. An equilibration step followed that consisted of molecular dynamics at 600 K for 10 ps. The resulting conformation was then subjected to 1 ns of molecular dynamics at 600 K, and snapshots of the conformations were taken every 1 ps to yield 1000 conformers. Each conformer was then subjected to conjugate gradient minimization until the RMS energy derivative was less than 0.0001 kcal Å^{-1}. These structures were screened further by rejecting any structures that were at least 5 kcal Å^{-1} greater than the global minimum for the assembly of structures. Further refinement was performed by validating the resulting structures of each compound using the NMR-derived restraints.

Acknowledgment. Financial support of this work by USDA-NRICGP Grant 99-35503-8231 is greatly appreciated. The NMR instrument was purchased with a grant from the Department of Energy (DEF6 0589346-0892).

Supporting Information Available: Ramachandran-type plots for dihedral angles depicted in Figure 2 (Figures S1−S6) and the complete set of NMR-derived restraints (Tables S1−S4) (PDF). This material is available free of charge via the Internet at http://pubs.acs.org.

JO035380W

(29) Dauber-Osguthorpe, P.; Roberts, V. A.; Osguthorpe, D. J.; Wolff, J.; Genest, M.; Hagler, A. T. *Proteins: Struct., Funct., Genet.* **1988**, *4*, 31−47.